The version of record is available at: https://doi.org/10.1088/2752-664X/adfa9e

Diurnal temperature range drives understory plant community composition in micro-climatically complex temperate montane forests

Authors: Adam L. Mahood^{1,*}, David M. Barnard¹, Jacob A. Macdonald¹, David W. Pittenger², Sarah M. Hall², Paula J. Fornwalt³

Affiliations:

- 1. Water Resources Systems Management, USDA-ARS, Fort Collins, CO
- 2. Valles Caldera National Preserve, National Park Service, Jemez Springs, NM
- US Department of Agriculture, Forest Service, Rocky Mountain Research Station, Fort Collins, CO

Keywords: cold air drainage, diurnal temperature range, microclimate, plant ecology, topography, vapor pressure deficit

Abstract

Cold air drainage is common in mountains, and leads to large, fine-scale differences in diurnal temperature range (DTR). DTR is hypothesized to drive plant community assembly, because areas with high DTR can be exposed to both extreme high and extreme low temperatures in the same day. We established networks of temperature and relative humidity sensors along DTR gradients in two montane forest basins, and conducted plant surveys around each sensor (n=45). We studied the seasonal stability of DTR and its effects on fine-scale variation in plant community composition; and used topographic metrics to create spatial models of DTR.

We found that mean DTR was stable throughout the year, although it was more variable around the mean (i.e., the standard deviation was higher) in winter months. It achieved both time series stability and distinguishability in less than 100 days, and was most strongly associated with daily minimum vapor pressure deficit. DTR measured *in situ* was the only variable that explained more than 50% of the within-basin variation in species composition for both basins, but among basins coarser-scale climatic variables (actual evapotranspiration, topographic wetness index, and climatic water deficit) performed better. DTR had a small, negative effect on species richness. Our simple model of DTR explained 64% of the variation, using only topographic wetness index and elevation as predictors.

These findings illustrate how at broad scales, average temperature and moisture conditions drive the regional species pool, but fine scales distribution of plant species within a basin is driven by microclimate. Accounting for fine-scale topoclimatic processes will lead to better models that capture topoclimate gradients, allowing for improved representation of complex

^{*} Corresponding author: admahood@duck.com

ecological processes in earth systems models. Future studies should account for microclimate, especially DTR, when designing experiments as sampling across microclimates will introduce bias into community observations.

Introduction

Identifying microclimatic refuges from high temperatures is emerging as an important strategy for mitigating the impact of shifting weather patterns on species diversity. Because fine-scale variation in microclimate is much greater than coarse-scale variation in macroclimate, species do not necessarily need to track broad-scale climatic shifts to find a suitable refuge from increasing temperatures (Maclean and Early, 2023). Large differences in species composition across small distances have been attributed to microrefugia—localized areas that are systematically colder than the surrounding landscape (Finocchiaro *et al.*, 2023), with stable microclimatic conditions (Ashcroft and Gollan, 2013) that can be partially decoupled from the surrounding macroclimate (Finocchiaro *et al.*, 2024). These systematically colder topographic depressions also serve as fire refugia (Rodman *et al.*, 2023), so identifying these locations is doubly important. But while changing the scale of analysis to a finer resolution can improve predictions, the variables which are relevant as drivers of community composition may also change. The same bioclimatic variables that explain the composition of regional species pools may not be as meaningful when examining fine-scale species occurrence, because orographic processes drive highly variable conditions at the boundary layer at these scales (Mahrt, 2022).

A common orographic process that creates stable areas of systematically colder air temperatures decoupled from bulk conditions is cold air drainage (CAD) (Mahrt, 2006, 2022; Ashcroft and Gollan, 2013). Cold air drainage events occur mainly on nights with low wind speeds, when colder, denser air flows down hill and accumulates in low lying areas. This creates areas that are systematically colder at night than the surrounding landscape. Meanwhile, daytime temperatures in these low lying areas deviate less from temperatures in surrounding areas, resulting in large diurnal temperature ranges (DTR, the difference between daily maximum (T_{max}) and minimum temperatures (T_{min})). The more area upslope to a given location, the more cold air it receives, and the lower the nighttime low becomes (Dobrowski et al 2009). But these places are also at lower elevations, so they have higher daily maximum temperatures. More ridgeward positions have lower daytime highs, but they also have higher nighttime lows, because after sundown katabatic flows carry colder, denser air downhill to valley bottoms, which is then replaced by less dense, warmer air (Figure 1). This results in temperature decreasing more slowly on ridgelines after sunset as cold air descends through gullies and pools in the valley. So while temperatures are expected to increase somewhat uniformly across scales as climate warms, the role of orographics in driving finer-scale patterning of climatic variability, especially in complex terrain, will remain constant (Dobrowski, 2011). Therefore the locations that export and receive cold air via CAD, and thus will have low and high DTR, respectively, will have consistent deviations from bulk conditions.

Diurnal temperature range is likely to be a key driver of plant community assembly (Gallou *et al.*, 2023), since both high and low temperatures can act as environmental filters on plant

occurrence and thus community assembly (Keddy and Laughlin, 2021). Frequent exposure to heat, drought and cold stress may therefore result in "range squeeze", with fewer species that are able to persist in such an environment (Bai et al., 2019; Gallou et al., 2023). High temperatures can cause heat stress and exacerbate drought stress (Ruehr et al., 2015; Guha et al., 2018; Marchin et al., 2022). Colder temperatures limit which plant species can persist based on frost tolerance, photosynthetic pathways, and freeze-thaw stress (Manasa S et al., 2022). Places with frequent temperature inversions have been found to have inverted patterns in forest composition, in some cases causing a 'reverse treeline' phenomenon (Coop and Givnish, 2007a; Pastore et al., 2024). Diurnal temperature range can also drive differences in plant morphology (Myster and Moe, 1995; Mu et al., 2022), growing season phenology (Barnard, Barnard and Molotch, 2017; Huang et al., 2020) and shifts in DTR due to climate change are expected to favor competitive dominance of non-native plants (Chen et al., 2017). Therefore, given the ubiquity of CAD, and that DTR appears to have a strong effect on plant community assembly, it is likely that many plant species may be adapted to grow in high or low DTR environments rather than tracking mean, minimum or maximum temperatures alone (Finocchiaro et al., 2024).

It is becoming increasingly clear that fine-scale (<= 10m) measurements are necessary to truly capture fine-scale conditions and processes that shape ecosystem functioning (Kemppinen et al., 2024; Klinges et al., 2024). Diurnal temperature range is one such phenomena that is driven by different processes at fine scales than it is at coarse scales. Coarse-scale variation in DTR is primarily driven by aridity (Wang et al., 2014; Sun et al., 2019). Water vapor has a high specific heat and thus moderates daily temperature maximums while also carrying higher temperatures into the night. More arid areas also have a higher sunshine duration, which drives higher maximum daily temperatures, and less arid areas have higher soil moisture which dampens increases in T_{max} via evaporation (Wang et al., 2014). Fine-scale variation DTR driven by CAD is not well captured by coarse-scale gridded climate products. Comparisons of in situ measurements against modeled data found that DTR is substantially underestimated even in grasslands with flat, simple topography (Bernath-Plaisted et al., 2023). Even if daily gridded T_{max} and T_{min} are used to calculate DTR from coarse-scale gridded products, the degree of DTR inaccuracy in gridded products is likely a function of topographic complexity within a given pixel. Without in situ training data, process-based models that can generate sub-daily microclimate estimations at fine resolutions are preferred for estimating fine-scale orographic processes (Maclean, Mosedale and Bennie, 2019; Maclean and Klinges, 2021; Kemppinen et al., 2024). Many modeling methods are now available, with a variety of approaches and levels of detail, that can incorporate CAD into sub-daily, high-resolution temperature estimates (Maclean, Mosedale and Bennie, 2019; Maclean and Klinges, 2021) from which DTR can be derived, but there are no out-of-the box gridded estimations of fine-scale DTR that we are aware of that currently available at a spatial resolution (<= 10 m) that captures the phenomenon.

Here, we measured fine-scale temperature and relative humidity, along with plant community composition at 46 locations in two western US study sites of similar temperate forest ecosystems. Each study site constituted a single basin, with cold air drainage events flowing downslope from higher elevation ridges to the valley bottom. One site, Valles Caldera National

Preserve in New Mexico, is a wide, round basin that receives cold air from the surrounding mountains, while the other, Manitou Experimental Forest in Colorado, consists of low-lying river valley with ridgelines to the east and west consisting of narrow gulches that funnel CAD to the valley bottom (Figure 1). Our overarching theory is that CAD-driven DTR is an important and stable facet of microclimate/refugia, and a key driver of community assembly. Because CAD is analogous to water movement in complex terrain, generally flowing downhill and pooling in low-lying areas, geospatial estimates of topographic position such as the Topographic Wetness Index (TWI) (Beven and Kirkby, 1979) can be used to understand and predict CAD-driven DTR. In this regard, we were interested in three research questions. 1) How does CAD-driven DTR vary through space and time, how stable is it, and what other microclimatic variables are associated with it? 2) How does fine-scale variation in microclimate, including DTR, affect plant community composition and diversity? 3) How strongly associated with plant communities are these microclimatic variables compared to commonly used coarse-scale, gridded estimations? We hypothesized that (1) DTR would be stable throughout the year, and negatively associated with T_{min}; (2) DTR would be a key driver of plant community composition and that sites with higher DTR would have lower diversity; and (3) that climate metrics that are typically used in coarse-scale species distribution models would work well at distinguishing among basins since those are the drivers of the composition of regional species pools, but within a basin, fine-scale metrics associated with CAD would distinguish between communities since those processes drive local heterogeneity in climate. Finally, researchers may benefit in incorporating fine-scale DTR variation into ecological modeling frameworks, but often do not have the time or resources to measure fine-scale DTR for months. Therefore, we explored how to create simple models of DTR at the 10 m scale from publicly available data topography data.

Methods

Study Basins

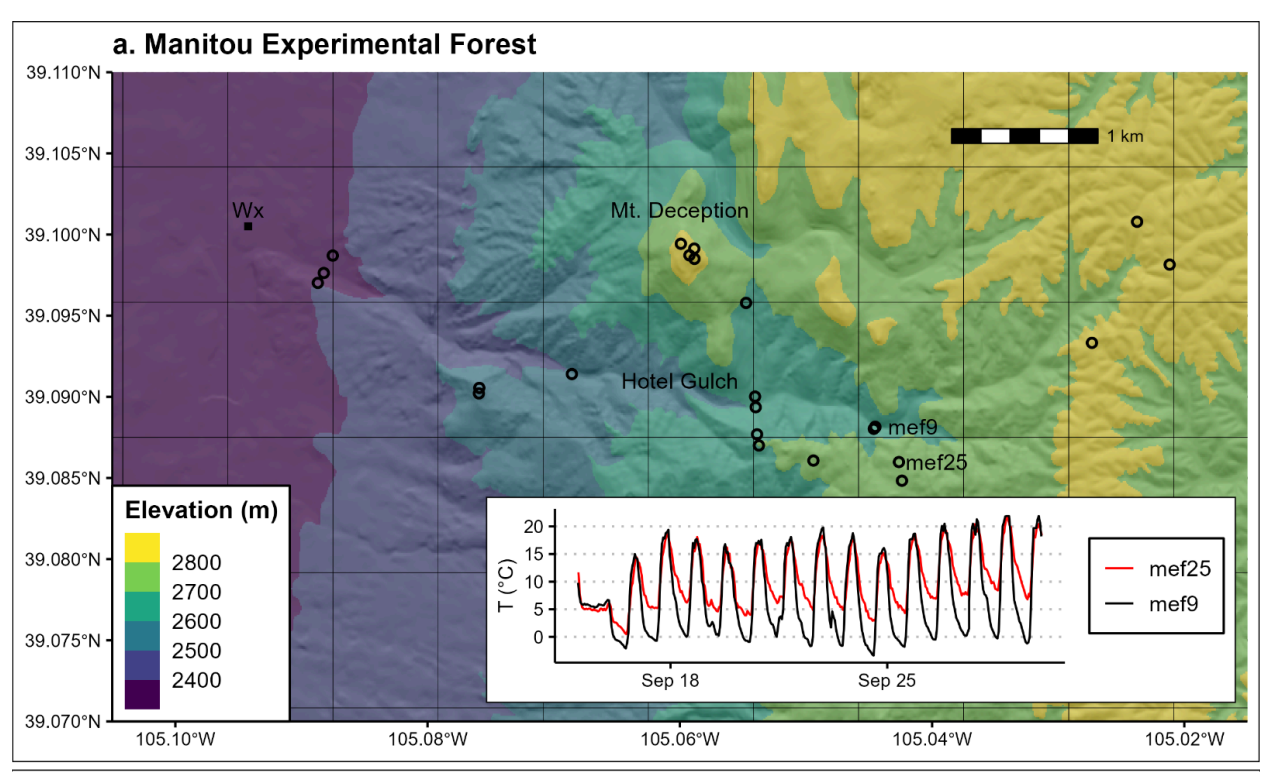
Manitou Experimental Forest

The first study basin was within the Manitou Experimental Forest (hereafter, Manitou) in central Colorado (Adams, Loughry and Plaugher, 2008). Manitou is a 6,758 ha research facility that ranges from 2,286 to 2,835 m in elevation. Its highest elevations occur near its eastern border, which follows a broad ridgeline. Gulches flow downhill from east to west off the ridgeline. It has a semi-arid, hemiboreal climate, with approximately 400 mm of precipitation falling annually and with annual temperatures averaging around 5.5 °C (Frank et al., 2021). The soils are granitic, coarse, and generally low in organic matter. Much of Manitou is covered by ponderosa pine (*Pinus ponderosa*) and ponderosa pine - Douglas-fir (*Pseudotsuga menziesii*) forests. Dry and mesic mixed conifer forests (generally composed of mixtures of ponderosa pine, Douglas-fir, lodgepole pine (*Pinus contorta*), limber pine (*Pinus flexilis*), and blue spruce (*Picea pungens*)) and lodgepole pine forests are prevalent in gulches and at the highest elevations. Understories tend to be a diverse mixture of graminoids, forbs, and low-growing shrubs, but can be depauperate in areas of high forest cover. We installed sensors and conducted plant surveys

(described below) at locations along the top of the eastern ridgeline, and in and above Hotel Gulch, which flows off the ridgeline (**Fig 1a**). We also installed sensors and conducted plant surveys at the top of Mount Deception, the highest point on the Experimental Forest, and 50-100 m downhill from the summit of Mount Deception in the cardinal directions.

Valles Caldera National Preserve

The second study basin was Valle Grande, part of the 35,977 ha Valles Caldera National Preserve (hereafter, Valles Caldera) in northern New Mexico. Valles Caldera is a resurgent caldera with an uplifted valley floor. It has a semi-arid, hemiboreal climate, with 600 mm of precipitation falling annually, and an average yearly temperature of 5.4 °C (Western Regional Climate Center, 2024). Elevation ranges from 2,500 to 3,400 m. This study area is characterized by dome-shaped mountains called cerros that were created by a series of volcanic eruptions over the last 1.23 million years. Soils of the slopes of the cerros and volcanic features are well-drained rhyolite and dacite flow rock, with welded and non-welded ash flow. Between the cerros are wide valleys formed from ancient lake sediments. Soils here are loamy and have varying degrees of organic matter, depending on groundwater availability (Valles Caldera Trust, 2011). At the highest elevations of the preserve (above 3.050 m) are spruce-fir forests dominated by Engelmann spruce (Picea engelmannii) and corkbark fir (Abies lasiocarpa var. arizonica) (Muldavin and Tonne, 2003). Below spruce-fir forests and starting at approximately 2,750 m are dry and mesic mixed conifer forests, generally co-dominated by fir and pine species: Douglas-fir, white fir (Abies concolor), blue spruce, southwestern white pine (Pinus strobiformis), limber pine, and ponderosa pine. Ponderosa pine forests appear below mixed conifer forests on the elevational gradient, and above montane grasslands. Montane grasslands can be found at different elevational gradients throughout the Preserve but the lower elevation grasslands occupy the largest area. Upland bunchgrasses dominate this community, but scattered trees or shrubs can be found in areas of infrequent fire. Montane wet meadows and wetlands occur throughout the lowland valleys, commonly adjacent to perennial streams of the valley bottoms, but also along seeps, springs, and creeks in the uplands. These diverse communities are dominated by facultative and obligate wetland graminoid species, mostly sedges (Carex spp.) and rushes (Juncus spp). We installed a transect of sensor and plant survey locations traversing between high points across the valley floor, with four additional locations in areas we assumed would receive substantial CAD (Fig 1b). Only one of our locations was at the edge of a wet meadow, and none were in grasslands or wetlands, so the locations at the valley bottom are still representative of the lower end of the ponderosa pine forest zone. Valles Caldera has a well-documented reverse treeline phenomenon, where tree establishment at the valley floor is limited by low temperatures (Coop and Givnish, 2007a, 2007b, 2008). Manitou, in contrast, does not exhibit the reverse treeline phenomenon.



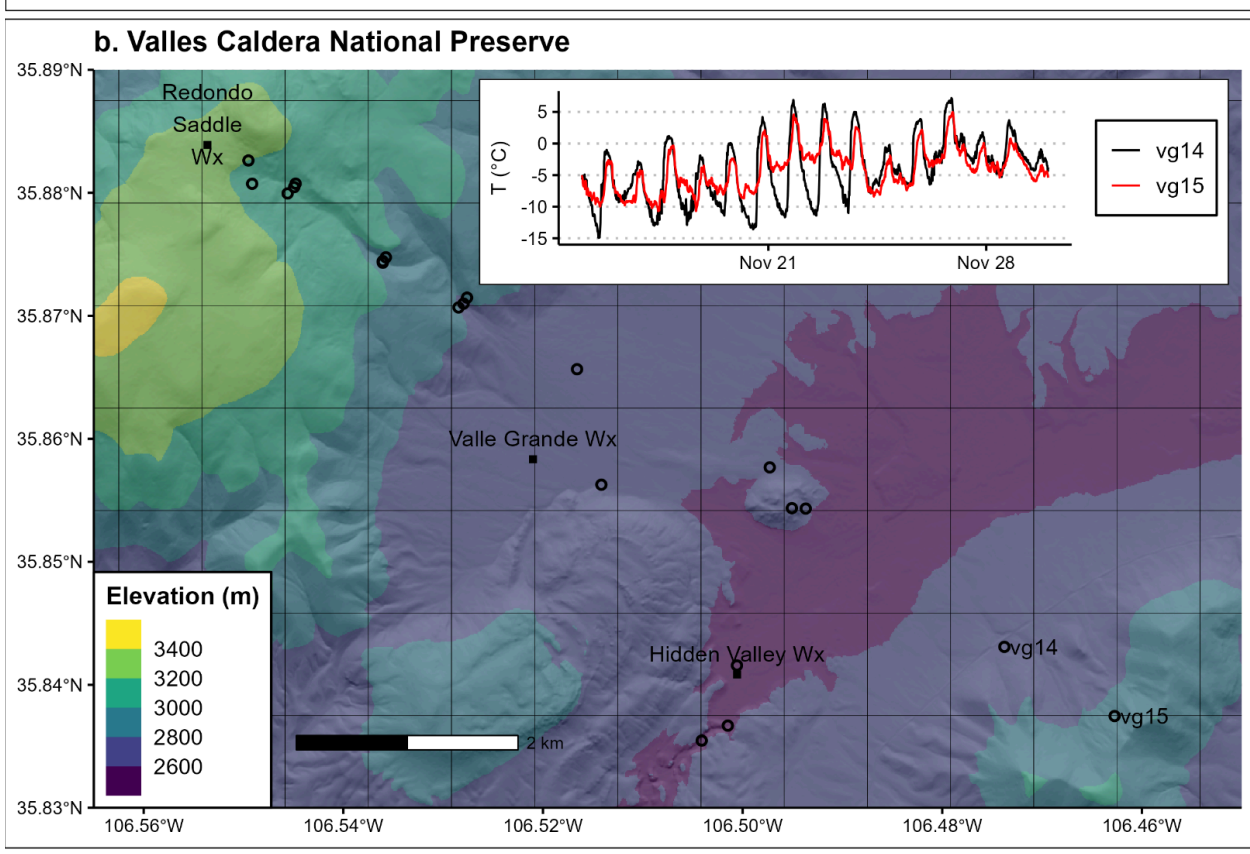


Figure 1: Map of the two study basins at (a.) the Manitou Experimental Forest, Colorado, and (b.) Valles Caldera National Preserve, New Mexico. Weather station (Wx) locations are represented as solid squares, and sensor locations are open circles. Rectangular outlines represent 800 m (30 second) PRISM grid cells. Some sensors were located very close to each other to capture aspect differences, so the points are overlapping on the map. The insets for each site show cold air drainage events at paired sensors, where the downhill sensor gets much colder on calm nights.

Data

In situ microclimate and plant survey measurements

We deployed small sensors (https://bluemaestro.com) that logged hourly temperature and relative humidity at 27 locations at Manitou and 21 locations at Valles Caldera (Fig 1). Each sensor was hung two meters above the ground, situated within a radiation shield made of 2 inch PVC pipe with diagonal ventilation slots cut in the sides with a circular saw (Supplemental Figure 1). Before field deployment, we conducted pilot tests of the sensors with PVC radiation shields by deploying them alongside a HOBO shielded temperature and humidity sensor, to ensure that the shields were effective (Supplemental Figure 1). These pilot tests revealed that the measurements taken under the PVC shields matched the HOBO sensors well with the exception of the hour of peak temperature, which was solved by hanging them on the north side of a tree. Sensors were deployed at the field locations for approximately 1 year at both basins. At Manitou, three of the sensors failed and the data were unrecoverable, leaving us with a total of 24 sensors from which to characterize microclimate. Due to instrument failure and difficult site access during the winter months, the Valles Caldera sensors only had about three months of data for most sensors (September - November), requiring us to quantify microclimate stability and distinguishability (described below) to assess how well those data represented year-round conditions. We used data from local weather stations (Frank et al., 2021; Western Regional Climate Center, 2024), as well as ERA5 data acquired via the R package mcera5 (Klinges et al., 2022), to validate and conduct quality assurance and control on the sensor data. We calculated hourly vapor pressure (VPD) deficit from temperature and relative humidity using the Clausius-Clapeyron equation. We then calculated the daily minimum, maximum, mean and range for temperature and VPD, and then we calculated the mean of the entire time series for each metric at each sensor.

In August 2023, we documented plant community composition around each microclimate sensor. We identified every plant species encountered within a five meter radius of the sensor, as long as the slope, aspect, curvature and other topographic conditions were the same as they were directly below the sensor. If there was, for example, an abrupt change in slope or aspect within the 5 m radius, we adjusted the center of the survey so as to not include that break in the slope. We calculated species richness as the number of species encountered.

Gridded climate data

We obtained three gridded datasets to compare how species associations with climate differed between our fine-scale sensor data and three sets of coarse-scale climate data products that are commonly used in studies of plant communities. The first was PRISM, an 800 m gridded climate reanalysis dataset (PRISM Climate Group, 2024). We used 30 year normals of maximum VPD (VPD_{max}), minimum VPD (VPD_{min}), T_{max}, T_{min}, mean annual precipitation, and mean annual temperature directly from PRISM, and we derived annual temperature range from T_{max} and T_{min} . The second was WorldClim, which is another climate reanalysis dataset that is produced at the same spatial resolution as PRISM. From WorldClim, we used the 30 year normal of DTR (Fick and Hijmans, 2017). The third dataset was TopoTerra (Hoecker et al., 2025). TopoTerra was derived from 4 km resolution TerraClimate (Abatzoglou et al., 2018) and downscaled to 240 m via the gradient-plus-inverse distance squared method (Flint and Flint 2012) using Topofire (Holden et al., 2019) as a template to capture fine-scale spatial variability in climatic water balance. TopoTerra is derived from a process-based model driven by topoedaphic features (aspect, slope angle, topographic position, soil water holding capacity). observations of biophysical variables (temperature, precipitation, insolation, and cloud cover) and explicitly includes CAD. We used 30 year normals of annual temperature range, T_{min}, T_{max}, actual evapotranspiration (AET) and climatic water deficit (CWD) from the TopoTerra dataset.

Gridded topography data

In order to characterize topography at the study locations, we acquired 10 m digital elevation models from the United States Geological Survey's National Elevation Dataset (Gesch *et al.*, 2002) and from these grids we calculated slope, aspect, topographic wetness index (TWI) (Beven and Kirkby, 1979), heat load index (HLI) (McCune and Keon, 2002), and folded aspect using the *terra* (Hijmans, 2023), *topomicro* (Mahood, 2024), and *spatialEco* (Evans and Murphy, 2023) R packages.

Statistical Analysis

Exploring the characteristics of diurnal temperature range

Because our sensor data was limited to three months (September - November) at Valles Caldera and 12 months at Manitou, we conducted a sensitivity analysis on two years of weather station data to assess seasonal variability in DTR in order to understand how much data would be required to be representative of the variation among sensors. We used data from three weather stations at Valle Grande, the largest basin in Valles Caldera. Each weather station was situated in a different topographic setting in relation to cold air drainage (**Figure 1b**). One was a donor of cold air, located at the saddle between Redondo Peak and Redondito at (elevation 3,260 m). One was a recipient of cold air, located at the mouth of Hidden Valley (2,500 m), where most of the cold air from the Valle Grande basin drains. The third, Valle Grande, was on the valley floor of Valle Grande, but upslope from Hidden Valley (2,620 m). It receives cold air from Redondo Peak and Redondito, but not from the entirety of the basin. In order to assess the stability of DTR at the three sites, we first selected a sample for 10 consecutive days and calculated the mean DTR, conducted an augmented Dickey-Fuller test using the *adf.test*

function from the *tseries* R package (Trapletti and Hornik, 2024) to assess the stability of the mean (Said and Dickey, 1984), and conducted a t-test between the three combinations of sites to assess our ability to distinguish between sites. We then increased the sample by one and repeated the process until we reached 600 days. Finally, we used linear models to assess how strongly associated DTR was with other microclimatic variables.

Plant community composition and species richness

We used non-metric multidimensional scaling (NMDS) ordinations (Minchin, 1987) to examine plant community composition. To create these ordinations, we used the *metaMDS* function in the *vegan* R package (Oksanen *et al.*, 2022), using a Bray-Curtis dissimilarity matrix. In order to understand how our *in situ* microclimate measurements, climate model predictions (see below), and gridded climate and topography data were associated with those ordinations, we ran a permutational correlation between the ordinations and climate and topography variables with 9,999 repetitions (the *envfit* function; (Oksanen *et al.*, 2022)).

During our exploratory analysis, our ordinations suggested that plant communities sorted themselves on either side of a threshold of DTR, rather than along a smooth gradient. Therefore, we decided to classify sensor locations as either donors or receivers of CAD and then use that threshold to test how being a receiver or donor of CAD affected species richness. In order to quantify a DTR threshold, we chose a range of threshold values between 10 and 20 °C, and on each value ran a permutational analysis of variance (PERMANOVA; the *adonis2* function in the *vegan* R package) (Anderson and Walsh, 2013). A PERMANOVA is a non-parametric, multivariate permutation test, with the dissimilarity matrix created from species occurrence data as the response variable, and environmental variables as predictors. Here, each site was binned as a CAD donor if the average DTR was below the threshold value, and a CAD recipient if it was above the threshold value. Because this threshold may differ by region, we determined separate thresholds for each basin. We considered the best thresholds to be those with the highest the R² values for the threshold value.

In order to test our hypothesis that CAD recipients would have lower diversity than CAD donors, we fit a generalized linear model in a Bayesian framework using the R package *brms* (Bürkner, 2017) with species richness as the dependent variable with a Poisson error distribution. Basin (Valles Caldera or Manitou), and whether the average DTR at the sensor station was above or below the threshold (CAD donor or recipient), were predictor variables. Model fit was assessed via Bayesian R² (Gelman *et al.*, 2019) using the *performance* R package (Lüdecke *et al.*, 2021).

Because CAD donors and recipients are also associated with higher and lower elevations, respectively, we constructed a structural equation model (SEM) to explore these causal pathways and rule out the contrasting idea that species richness was really only associated with soil moisture (with TWI as a proxy) or elevation. We created two generalized linear models, one with species richness as the poisson-distributed response and DTR, TWI and elevation as the predictors. The second model had DTR as the gaussian-distributed response and elevation and TWI as the predictors. We then used the R package piecewiseSEM to combine those models into an SEM (Lefcheck 2016).

Modeling diurnal temperature range

We used spatial process models to estimate DTR at the study basins from 10 m digital elevation models. We selected predictor variables by creating linear models with a range of topographic predictors: slope, folded aspect, HLI, TWI, elevation, and relative elevation (elevation - minimum elevation of the basin). We explored modeling both basins together and separately, and settled on the most parsimonious model using AICc. We used the *performance* R package to visually check model assumptions (normality of residuals, normality of random effects, linear relationship, homogeneity of variance, multicollinearity) (Lüdecke *et al.*, 2021). In order to also account for spatial autocorrelation, we fit a spatial process model using the *fields* R package (Nychka *et al.*, 2021) using the same predictors, and used that model to create gridded predictions of DTR at both sites. We used Leave one out cross validation to assess predictive accuracy for the spatial process model.

All analysis was done in R (R Core Team, 2021). Data and code are provided at www.github.com/admahood/microclimate-veg (Mahood, 2025).

Results

Diurnal temperature range at reference sites was stable throughout the year, and more strongly associated with VPD_{min} than T_{min}

Mean DTR was relatively stable throughout the year at the three Valles Caldera weather stations (**Figure 2a & d**). Variation in DTR was higher during the winter months, especially at Hidden Valley, the location receiving cold air from the entire valley. Data from the Valles Caldera weather stations indicated that the time series of diurnal temperature range became stable in 100 days or less (**Figure 2b**). Consistently finding significant differences between sites required less than 60 days at the p < 0.05 level (**Figure 2c**). Therefore, given that DTR stability was reached within roughly 3 months and DTR distinguishability within 2 months, we argue that three months is sufficient to capture differences among sites. At fine scales, mean DTR at our microclimate sensor locations had a mean of 13.6 °C and ranged from 8.6 to 20.4 °C at Manitou, and had a mean of 12.2 °C and ranged from 7.1 to 18.1 °C at Valles Caldera. Diurnal temperature range at our weather stations and microclimate sensor locations had a strong negative relationship with average daily VPD_{min} ($R^2 = 0.66$), more so than average daily T_{min} ($R^2 = 0.12$) (**Figure 3c**).

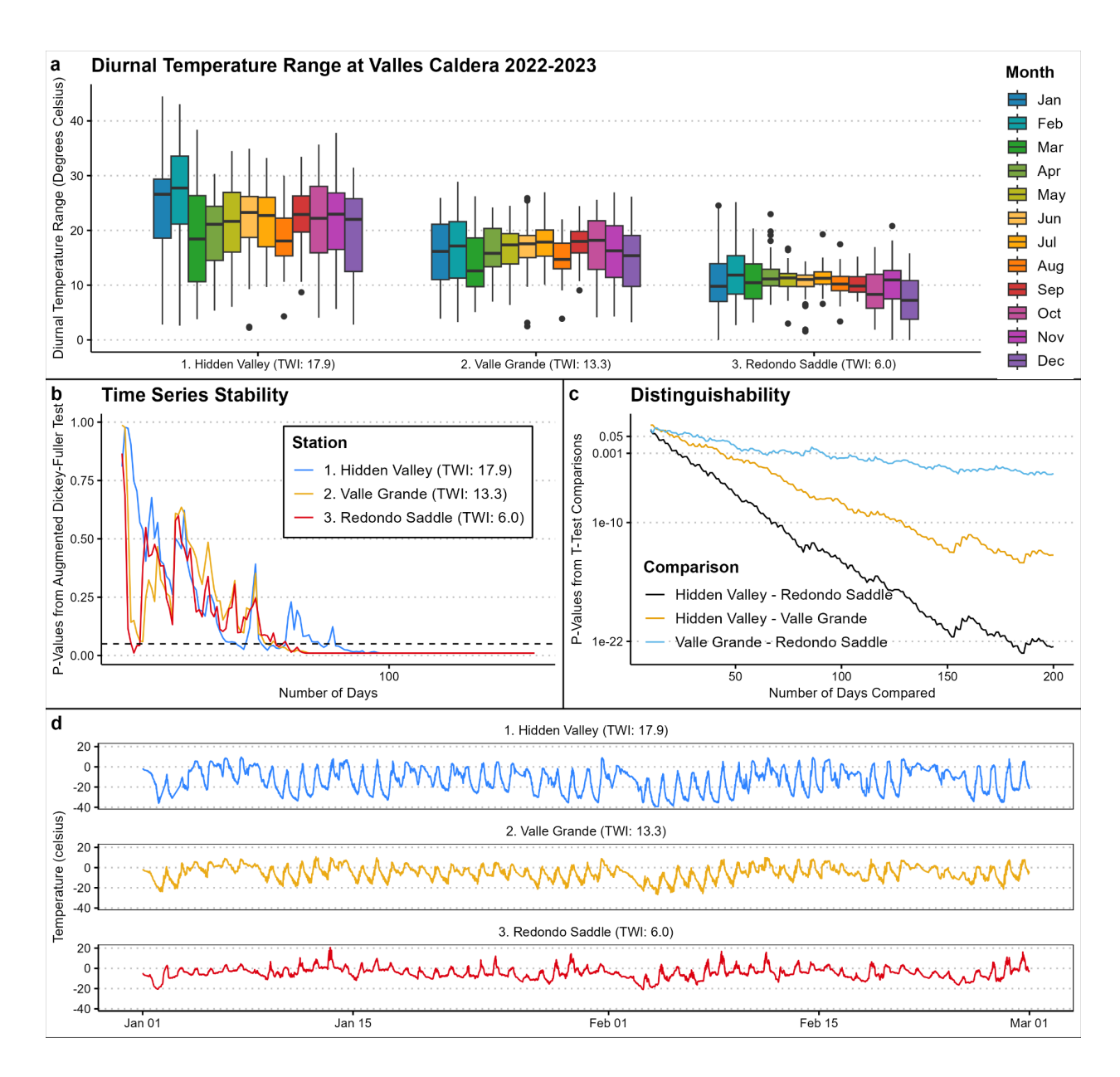


Figure 2: Exploration of the properties of cold air drainage-driven variation in diurnal temperature range (DTR). Mean DTR at three weather stations at Valles Caldera had minimal seasonal variability over two years (a). Augmented Dickey-Fuller tests showed the time series of DTR achieved stability in less than 100 days for all sites (b) and only two months of data was necessary to consistently find statistically significant differences between sites at the p < 0.05 level (c). Panel d is a time series for the first two months of 2022.

CAD-driven diurnal temperature range is associated with microscale community composition and diversity

In our plant surveys, we encountered 254 total species. We found 129 species at Manitou and 168 at Valles Caldera, with 42 species encountered at both basins. The most common understory species for both basins are given in Tables S1 and S2. Permutational correlations

showed that fine-scale DTR ($R^2 = 0.59$ at both sites) and VPD_{min} ($R^2 = 0.62$ at Manitou, 0.37 at Valles Caldera) were more strongly associated with the ordination than any other micro- or macro-climatic variable when basins were analyzed separately (Table 1). Communities at each site were grouped on either side of a basin-specific threshold in DTR (Figure 3). According to the PERMANOVA test, the threshold was estimated to be 14 °C for Valles Caldera (peak R2 = 16.8) and 15 °C for Manitou (peak R² = 21.0; **Figure 3**). Our model of diversity above and below the threshold was well-converged (R-hat = 1.0, ESS > 2000 for all coefficients), and showed a well-supported but small effect of higher diversity for CAD donors ($R^2 = 0.179$) (Figure 3b; **Table S3**). In our SEM analysis, the model was well-fit ($X^2 = 2.7$, p > 0.05; Fisher's C = 4.6, p >0.05). Diurnal temperature range as a continuous variable had a small, negative effect on species richness (p = 0.005), while relative elevation was not significant and TWI had a smaller but significant effect (p= 0.02). The standardised effect of DTR on species richness was 0.39 compared to 0.24 for TWI (Table S4), providing more evidence that DTR is affecting species richness rather than simply being correlated with elevation and soil moisture. In an examination of the species associations with basin-level ordinations, 17 species were strongly associated (R² > 0.4, p < 0.01), and 4 of those species were orthogonal to the DTR threshold (**Figure S2**). Pseudotsuga menziesii was the only species common to both basins that was significantly correlated with the ordination, and in both cases it was associated with low-DTR communities (Figure S2).

CAD-driven diurnal temperature range less important at broad scales

When NMDS was conducted on the two basins grouped together, fine-scale DTR was not significantly associated with composition (**Table 1**). Rather, 30 year normal water balance metrics of AET ($R^2 = 0.39$) and CWD ($R^2 = 0.77$) modeled at coarser scales explained variation between the two basins, and 10 m TWI ($R^2 = 0.33$) and in situ average daily VPD_{min} ($R^2 = 0.33$) explained community composition within sites. Only TWI and in situ measurements of VPD_{min} and diurnal range in VPD were significant for both within- and between- basin analyses (**Figure 3, Table 1**).

DTR can be modeled based on TWI and elevation

The most parsimonious and generalizable linear model of DTR had elevation and TWI as predictors, and included both basins. It had an adjusted R² of 0.64. Including the basin as a predictor was not statistically significant, indicating that this simple model may be more broadly generalizable. The leave one out cross-validation of the spatial process model had an R² of 0.58 and a root mean squared error of 2.22 °C (**Figure 4**).

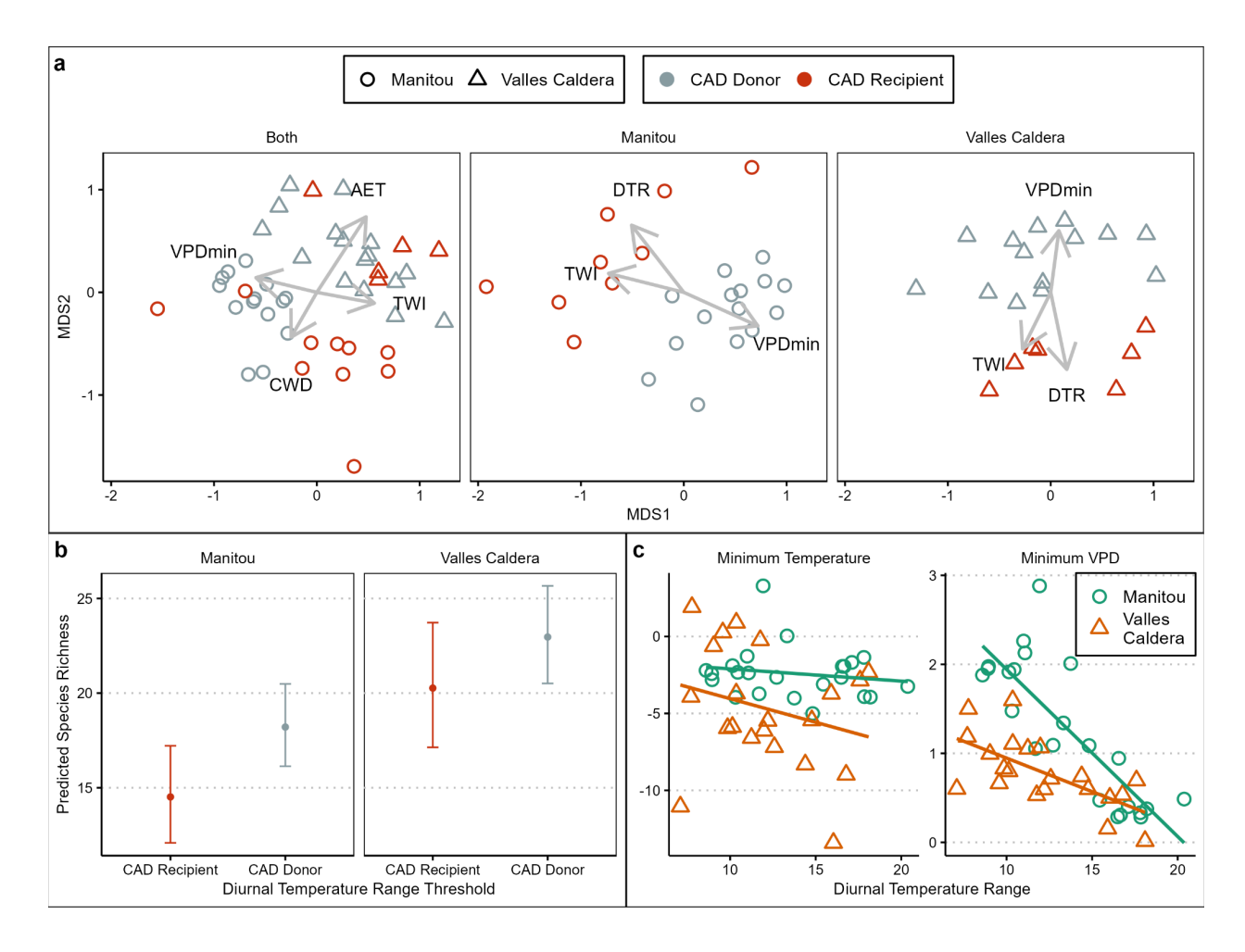


Figure 3: Panel a is a non-metric multidimensional scaling ordination on plant communities from both basins pooled together (left panel) and for each basin separately (right panel). Communities clearly separated along a threshold of diurnal temperature range (DTR) at both sites when ordinated separately, but not when the communities were pooled. Panel b shows the predicted species richness from a Bayesian hierarchical model, which was lower at both Manitou and Valles Caldera at locations over the DTR threshold. Panel c illustrates that DTR was more strongly associated with daily minimum VPD than with daily minimum temperature. Abbreviations: AET = actual evapotranspiration; CWD = climatic water deficit; TWI = topographic wetness index; DTR = Diurnal temperature range; VPDmin = average daily minimum vapor pressure deficit.

Table 1: Microclimate (in situ measurements) and macroclimate (coarser scale, gridded climate products) variables correlated with ordination. Only fine-scale diurnal temperature range measured *in situ* explained more than 50% of within-basin variation in composition at both basins, and the only other variable to explain more than 40% of within-basin variation in composition at both basins was modeled diurnal temperature range.

Variable	Source	Valles Manito Caldera		Both Basins
Diurnal Temperature Range	In situ	0.59 **	0.59 ***	0.01
Daily Minimum VPD ¹	In situ	0.37 *	0.62 ***	0.35 ***
Diurnal VPD Range	In situ	0.28 .	0.32 *	0.15 *
Daily Minimum Temperature	In situ	0.26 .	0.09	0.18 *
Daily Maximum VPD	In situ	0.21	0.16	0.21 **
Daily Maximum Temperature	In situ	0.18	0.19	0.11 .
Daily Mean Temperature	In situ	0.13	0.02	0.14 *
Daily Mean VPD	In situ	0.01	0.15	0.37 ***
Diurnal Temperature Range	Modeled (10 m)	0.44 **	0.42 **	0.02
Annual Temperature Range	PRISM (800 m)	0.62 ***	0.1	0.15 *
Maximum VPD	PRISM (800 m)	0.61 *** 0.19		0.17 *
Minimum VPD	PRISM (800 m)	0.56 **	0.06	0.22 **
Maximum Temperature	PRISM (800 m)	0.54 **	0.21 .	0.14 *
Minimum Temperature	PRISM (800 m)	0.52 **	0.35 *	0.08
Mean Annual Precipitation	PRISM (800 m)	0.51 **	0.17	0.16 *
Mean Annual Temperature	PRISM (800 m)	0.24 .	0.31 *	0.09
Annual Temperature Range	TopoTerra (240 m)	0.73 ***	0.15	0.24 **
Actual Evapotranspiration	TopoTerra (240 m)	0.52 **	0.17	0.75 ***

Maximum Temperature	TopoTerra (240 m)	0.43 **	0.2	0.09
Climatic Water Deficit	TopoTerra (240 m)	0.16	0.23 .	0.17 *
MInimum Temperature	TopoTerra (240 m)	0.12	0.27 **	
Elevation	Topography (10 m)	0.45 **	0.31 *	0.06
Relative Elevation	Topography (10 m)	0.45 **	0.31 *	0.14 *
Topographic Wetness Index	Topography (10 m)	0.38 *	0.56 ***	0.32 ***
Folded Aspect x Slope	Topography (10 m)	0.1	0.18	0.02
Heat Load Index	Topography (10 m)	0.04	0.02	0.14 *
Folded Aspect	Topography (10 m)	0.02	0.12	0.05
Diurnal Temperature Range	WorldClim (800 m)	0.59 ***	0.22 .	0.3 ***

^{1.}VPD = Vapor pressure deficit

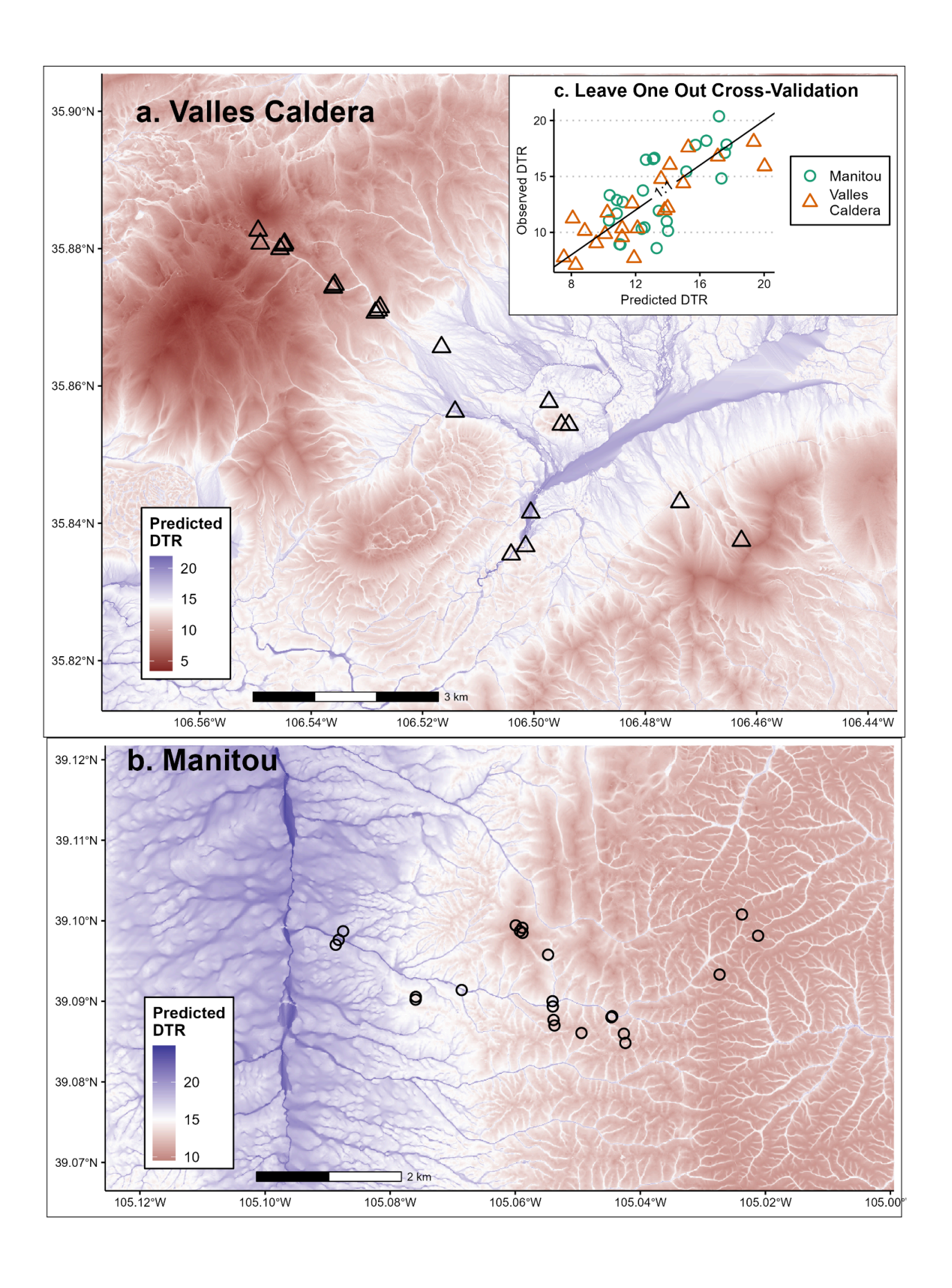


Figure 4. Spatial process model predictions of diurnal temperature range. In a and b, the midpoint of the color ramp, in white, corresponds to the thresholds from the prior figures. Observed vs predicted R^2 was 0.63 (c). Open shapes indicate microclimate sensor locations.

Discussion

We found that in two topographically complex basins with similar plant communities, plant community composition and species richness were strongly associated with fine-scale patterns in DTR. When the two basins were pooled for analysis, however, DTR was weakly associated with composition. Rather, between-basin composition was most strongly associated with coarse-scale estimations of AET. This aligned with our expectation that while the composition of regional species pools are driven by coarse-scale climatic conditions (Cornell and Harrison, 2014), fine-scale spatial variation within those species pools is driven by fine-scale processes including, but not limited to, CAD. We also found lower diversity in areas that were recipients of CAD and propose that the range squeeze hypothesis, wherein areas with high temperature ranges will have lower diversity because species have to be able to tolerate cold, heat and drought (Gallou *et al.*, 2023), is a plausible explanation.

When trying to understand the effect of CAD on biological communities, it may be more important to capture VPD_{min} and DTR, rather than T_{min}. Fine-scale variation in DTR was more strongly associated with minimum VPD than with minimum temperature (Figure 3c). Fine-scale variation DTR is driven by gravity, rather than aridity which drives DTR at coarser scales (Ashcroft and Gollan, 2013; Sun et al., 2019). Because cold air drains to the same places that water drains to, areas with high DTR driven by CAD have lower VPD, so modeling minimum temperature at fine scales may not fully capture the effect of CAD on biological communities. Much of the literature on CAD modeling is focused on modeling T_{min} and T_{max} (Dobrowski et al., 2009; Holden et al., 2011), and much of the microclimatic refugia work is focused on fine-scale variation in mean annual temperature and precipitation (Morelli et al., 2016; Maclean and Early, 2023). Vapor pressure deficit is a fundamental property of the atmosphere that is essential for understanding plant physiological responses to drought, as well as flammability and fire risk (Seager et al., 2015; Grossiord et al., 2020). The results presented here indicate an association between fine scale variation in VPD, and CAD-driven DTR. DTR has thus far been largely overlooked with some exceptions, and this is perhaps because most coarse scale products fail to capture that fine-scale variation in DTR. Because DTR has year-round mean stability and represents exposure to two temperature extremes, it may represent a fundamental quality of the provenance of microsites that needs to be accounted for when studying any ecosystem at fine scales.

DTR was one of the most strongly associated variables with community composition, and the only variable that performed well at both sites. It was, however, much less important between basins. Only fine-scale diurnal temperature range measured *in situ* explained more than 50% of within-basin variation in composition at both basins, and the only other variable to explain more than 40% of within-basin variation in composition at both basins was modeled diurnal temperature range. This result held true with DTR we estimated with spatial process models

(**Figure 5, Table 1**). Species that are not tracking coarse-scale gradients in elevation or latitude in their response to changing temperatures may be instead following fine-scale changes in topographically-driven variables like VPD_{min} and DTR. Some species may be specially adapted to both cold stress and drought stress, and so therefore would have a competitive advantage in high DTR areas, while for other species the two forms of physiological stress may limit their occurrence in those areas. If this is true, tracking their response to shifting weather patterns will require *in situ* plant sampling at high density, and high-resolution (5-10 m) estimates of microclimate (Patiño *et al.*, 2023). Moreover, the impact of DTR, and thus topography, as a driver of community assemblage needs to be considered when planning sampling campaigns in mountainous regions as a lack of sampling stratification across topographic positions will likely introduce a substantial amount of variation in community composition that would otherwise not be a factor if sampling among within similar DTRs.

High topographic complexity creates high microclimatic complexity which helps buffer against regional extirpations (Suggitt et al., 2018). But which topographic positions serve as microclimatic refugia is likely to be species-specific, and may or may not align with fire refugia. Species intolerant to extreme heat but tolerant of extreme cold may favor gullies or valley bottoms, where microclimatic refugia align with fire refugia. In these cases, refugia from fire and refugia from extreme maximum temperatures co-occur in CAD-receiving topographic positions (Rodman et al., 2023), because low nighttime VPD is the primary factor that limits fire spread at night (Balch et al., 2022). While CAD-receiving areas are more likely to be fire refugia, and they may also have more potential for productivity (Novick, Oishi and Miniat, 2016), they may not serve as plant biodiversity refugia since many plants are not adapted to high DTR (Gallou et al., 2023). Fire refugia are emerging as priorities for restoration efforts as temperatures increase (Rodman et al., 2023). Seedlings and recent transplants are highly vulnerable to temperature extremes, and so conducting successful restoration in these areas may present unique challenges that require creative approaches specific to the problems that daily temperature extremes represent. Other types of microclimatic refugia, such as springs, may serve as refugia from fire and for tree regeneration, but would not necessarily have the problem of high DTR in CAD-receiving areas.

While much of the current discussion centers around these low-lying areas with cooler mean temperatures as providing refuge from increasing temperatures, low-DTR areas on ridgeward positions may serve as a different type of microclimatic refugia—a refuge from both high and low temperature extremes. Non-generalist species that are intolerant to extreme cold may favor ridgeward positions (D'Odorico et al., 2013), which tend to burn at higher severity (Kane et al., 2015). In these cases, the microclimatic refugia and fire refugia do not align. Rare or threatened species that are both fire intolerant and prefer low-DTR areas may require special preparation for defense from fire, as those topographic positions are more vulnerable to high severity fire (Kane et al., 2015) and perhaps more difficult for firefighters to defend. Rare species that are adapted to these environments are disproportionately more at risk for local extirpation, especially in areas where changing fire regimes are likely to cause ecosystem type conversion (Keeley, van Mantgem and Falk, 2019; Mahood and Balch, 2019; Guiterman et al., 2022). Finally, since refugia are stable spatially (Platt, Chapman and Balch, 2024) and DTR is fairly

stable seasonally (**Figure 2**), those species that are adapted to high DTR may have a more positive outlook for persistence in a warmer world. Future studies on plant communities in topographically complex landscapes should be careful to stratify sampling according to microclimate variables like DTR that are driven by microtopographic position so as to not bias estimates of species composition and diversity (Fornwalt and Kaufmann, 2014).

Changes in DTR are expected with increasing greenhouse gas concentrations (Rupp *et al.*, 2021). The intensity of CAD events is expected to decrease by 10% by 2100 under an RCP 8.5 scenario (Rupp *et al.*, 2021), with warmer, more humid regions being the most at risk to changes in CAD. Because CAD-driven DTR is driven by orographic processes, the way it changes in response to increasing temperatures will likely be more spatially variable than the way that coarse-scale, aridity-driven DTR will. Coarse-scale estimations of DTR have been decreasing globally since the early 1950's, because nighttime minimum temperatures have been increasing faster than daytime highs (Braganza, Karoly and Arblaster, 2004; Lauritsen and Rogers, 2012; Sun *et al.*, 2019).

DTR was simple to model with only TWI and elevation. We expected elevation that was relativized to the basin to perform better when comparing across basins, but it did not (Adjusted R² = 0.51). This may be because mean temperature is driven by elevation, or because TWI already captures relative differences in elevation. We expect that when estimating DTR across broader areas encompassing more basins, elevation relativized to each basin will emerge as a necessary variable to capture DTR. It may be possible to use coarse products like PRISM or WorldClim to represent DTR, and then downscale, but it is important to note that simply subtracting the T_{min} from T_{max} of an annual or monthly mean is providing an annual or monthly temperature range, rather than DTR. Calculating monthly or annual temperature range without downscaling may adequately represent DTR in areas with coarse topography, because DTR is relatively stable throughout the year (Figure 2), but it will still fail in areas where the topography is more fine-scale than the climate data. But even areas with comparatively much more gentle topography than the mountainous areas here can have large fine-scale variations in temperature due to CAD (Mahrt, 2022). Caution must be taken, since capturing fine-scale variation in DTR likely requires fine-scale topographic data in areas like Manitou with complex topography, while areas like Valles Caldera with smoother topographic features may not require data of such high-resolution (Kemppinen et al., 2024). Furthermore, directly using topographic variables that drive microclimate as predictors of ecological responses may not be an effective way to represent the effect of microclimate on communities (Man et al., 2022). Rather, one should use topography to model microclimate, and then use the modeled microclimate to understand communities (Mahood et al., 2024).

Conclusions

Microclimatic variation driven by orographic processes is a key driver of fine-scale variation in species distributions, and the particular ways in which these fine-scale processes manifest to affect species distribution is poorly understood. As the field of microclimate modeling continues to develop, it will be important to explore how different aspects of microclimatic variation drive

ecological processes. Variables that are key drivers of coarse-scale variation in ecosystem composition and function may not be predictive of species occurrence at finer scales, and vice versa. Here, DTR was found to shape community composition at fine scales, but more research is needed to understand how general this phenomenon is. Other abiotic variables are also strong drivers of composition and diversity, but here we focus on DTR as it is a stable indicator of microsite provenance, but rarely included in ecological analyses. Fine-scale DTR appears to be straightforward to estimate from publicly available data and add to analysis workflows. Species distribution models relying on mean annual temperature and precipitation, even at fine scales, may not be well-suited to predict how species will respond to future changes in climate (Maclean and Early, 2023). Species adapted to low diurnal temperature range may have optimum microclimatic niches that lie on ridgelines or other fire-prone topographic positions, since those topographic positions have lower DTR. These species should be prioritized for monitoring and special attention during fire suppression. Land managers and scientists should focus on identifying species with habitat preferences where microrefugia and fire refugia do and do not match, in order to more effectively identify priority areas for both plant community restoration and fire suppression resources.

Acknowledgements

We thank Tyler Hoecker, and Jeffrey Chandler for data access and Steve Alton for logistical assistance. This work could not have been done without invaluable assistance in the field from Shanthini Ode, Maddy Guimond, Ross Shipley, Benjamin Stout, Mahika Rao and Riley Scaff. This research was conducted under National Park Service Scientific Research and Collecting Permit #VALL-2022-SCI-0017, and supported by the U.S. Department of Agriculture, Agricultural Research Service. The findings and conclusions in this publication are those of the authors and should not be construed to represent any official USDA or U.S. Government determination or policy. USDA is an equal opportunity provider and employer. This publication was written and prepared by US Government employees on official time, and therefore it is in the public domain and not subject to copyright.

References

Abatzoglou, J.T. *et al.* (2018) 'TerraClimate, a high-resolution global dataset of monthly climate and climatic water balance from 1958–2015', *Scientific Data*, 5(1), p. 170191. Available at: https://doi.org/10.1038/sdata.2017.191.

Adams, M.B., Loughry, L. and Plaugher, L. (2008) *Experimental Forests and Ranges of the USDA Forest Service*. Revised. Gen. Tech. Rep. NE-321. Newton Square, PA: U.S. Department of Agriculture, Forest Service, Northern Research Station, p. 183. Available at: https://doi.org/10.2737/NE-GTR-321.

Anderson, M.J. and Walsh, D.C.I. (2013) 'PERMANOVA, ANOSIM, and the Mantel test in the face of heterogeneous dispersions: What null hypothesis are you testing?', *Ecological Monographs*, 83(4), pp. 557–574. Available at: https://doi.org/10.1890/12-2010.1.

Ashcroft, M.B. and Gollan, J.R. (2013) 'Moisture, thermal inertia, and the spatial distributions of

near-surface soil and air temperatures: Understanding factors that promote microrefugia', *Agricultural and Forest Meteorology*, 176, pp. 77–89. Available at: https://doi.org/10.1016/j.agrformet.2013.03.008.

Bai, C.-M. *et al.* (2019) 'Independent and combined effects of daytime heat stress and nighttime recovery determine thermal performance', *Biology Open*, p. bio.038141. Available at: https://doi.org/10.1242/bio.038141.

Balch, J.K. *et al.* (2022) 'Warming weakens the night-time barrier to global fire', *Nature*, 602(7897), pp. 442–448. Available at: https://doi.org/10.1038/s41586-021-04325-1.

Barnard, D.M., Barnard, H.R. and Molotch, N.P. (2017) 'Topoclimate effects on growing season length and montane conifer growth in complex terrain', *Environmental Research Letters*, 12(6), p. 064003. Available at: https://doi.org/10.1088/1748-9326/aa6da8.

Bernath-Plaisted, J.S. *et al.* (2023) 'Microclimate complexity in temperate grasslands: implications for conservation and management under climate change', *Environmental Research Letters*, 18(6), p. 064023. Available at: https://doi.org/10.1088/1748-9326/acd4d3.

Beven, K.J. and Kirkby, M.J. (1979) 'A physically based, variable contributing area model of basin hydrology / Un modèle à base physique de zone d'appel variable de l'hydrologie du bassin versant', *Hydrological Sciences Bulletin*, 24(1), pp. 43–69. Available at: https://doi.org/10.1080/02626667909491834.

Braganza, K., Karoly, D.J. and Arblaster, J.M. (2004) 'Diurnal temperature range as an index of global climate change during the twentieth century', *Geophysical Research Letters*, 31(13), p. 2004GL019998. Available at: https://doi.org/10.1029/2004GL019998.

Bürkner, P.-C. (2017) 'brms: An R Package for Bayesian Multilevel Models Using Stan', Journal of Statistical Software, 80(1). Available at: https://doi.org/10.18637/jss.v080.i01.

Chen, B.-M. *et al.* (2017) 'Differential responses of invasive and native plants to warming with simulated changes in diurnal temperature ranges', *AoB PLANTS*, 9(4). Available at: https://doi.org/10.1093/aobpla/plx028.

Coop, J.D. and Givnish, T.J. (2007a) 'Gradient analysis of reversed treelines and grasslands of the Valles Caldera, New Mexico', *Journal of Vegetation Science*, 18(1), pp. 43–54. Available at: https://doi.org/10.1111/j.1654-1103.2007.tb02514.x.

Coop, J.D. and Givnish, T.J. (2007b) 'Spatial and temporal patterns of recent forest encroachment in montane grasslands of the Valles Caldera, New Mexico, USA', *Journal of Biogeography*, 34(5), pp. 914–927. Available at: https://doi.org/10.1111/j.1365-2699.2006.01660.x.

Coop, J.D. and Givnish, T.J. (2008) 'CONSTRAINTS ON TREE SEEDLING ESTABLISHMENT IN MONTANE GRASSLANDS OF THE VALLES CALDERA, NEW MEXICO', *Ecology*, 89(4), pp. 1101–1111. Available at: https://doi.org/10.1890/06-1333.1.

Cornell, H.V. and Harrison, S.P. (2014) 'What Are Species Pools and When Are They Important?', *Annual Review of Ecology, Evolution, and Systematics*, 45(1), pp. 45–67. Available at: https://doi.org/10.1146/annurev-ecolsys-120213-091759.

Dobrowski, S.Z. *et al.* (2009) 'How much influence does landscape-scale physiography have on air temperature in a mountain environment?', *Agricultural and Forest Meteorology*, 149(10), pp. 1751–1758. Available at: https://doi.org/10.1016/j.agrformet.2009.06.006.

Dobrowski, S.Z. (2011) 'A climatic basis for microrefugia: the influence of terrain on climate', *Global Change Biology*, 17(2), pp. 1022–1035. Available at: https://doi.org/10.1111/j.1365-2486.2010.02263.x.

D'Odorico, P. *et al.* (2013) 'Vegetation–microclimate feedbacks in woodland–grassland ecotones', *Global Ecology and Biogeography*, 22(4), pp. 364–379. Available at: https://doi.org/10.1111/geb.12000.

Evans, J.S. and Murphy, M.A. (2023) *spatialEco*. Available at: https://github.com/jeffreyevans/spatialEco.

Fick, S.E. and Hijmans, R.J. (2017) 'WorldClim 2: new 1-km spatial resolution climate surfaces for global land areas', *International Journal of Climatology*, 37(12), pp. 4302–4315. Available at: https://doi.org/10.1002/joc.5086.

Finocchiaro, M. *et al.* (2023) 'Bridging the gap between microclimate and microrefugia: A bottom-up approach reveals strong climatic and biological offsets', *Global Change Biology*, 29(4), pp. 1024–1036. Available at: https://doi.org/10.1111/gcb.16526.

Finocchiaro, M. *et al.* (2024) 'Microrefugia and microclimate: Unraveling decoupling potential and resistance to heatwaves', *Science of The Total Environment*, 924, p. 171696. Available at: https://doi.org/10.1016/j.scitotenv.2024.171696.

Fornwalt, P.J. and Kaufmann, M.R. (2014) 'Understorey plant community dynamics following a large, mixed severity wildfire in a *P inus ponderosa — P seudotsuga menziesii* forest, C olorado, USA', *Journal of Vegetation Science*. Edited by B. Collins, 25(3), pp. 805–818. Available at: https://doi.org/10.1111/jvs.12128.

Frank, J.M. *et al.* (2021) 'Manitou Experimental Forest hourly meteorology data (3rd Edition). Fort Collins, CO: Forest Service Research Data Archive.' Available at: https://doi.org/10.2737/RDS-2011-0001-3.

Gallou, A. *et al.* (2023) 'Diurnal temperature range as a key predictor of plants' elevation ranges globally', *Nature Communications*, 14(1), p. 7890. Available at: https://doi.org/10.1038/s41467-023-43477-8.

Gelman, A. *et al.* (2019) 'R-squared for Bayesian Regression Models', *The American Statistician*, 73(3), pp. 307–309. Available at: https://doi.org/10.1080/00031305.2018.1549100.

Gesch, D. et al. (2002) 'The national elevation dataset', *Photogrammetric engineering and remote sensing*, 68(1), pp. 5–32.

Grossiord, C. *et al.* (2020) 'Plant responses to rising vapor pressure deficit', *New Phytologist*, 226(6), pp. 1550–1566. Available at: https://doi.org/10.1111/nph.16485.

Guha, A. *et al.* (2018) 'Differential ecophysiological responses and resilience to heat wave events in four co-occurring temperate tree species', *Environmental Research Letters*, 13(6), p.

065008. Available at: https://doi.org/10.1088/1748-9326/aabcd8.

Guiterman, C.H. *et al.* (2022) 'Vegetation type conversion in the US Southwest: frontline observations and management responses', *Fire Ecology*, 18(1), pp. 6, s42408-022-00131-w. Available at: https://doi.org/10.1186/s42408-022-00131-w.

Hijmans, R.J. (2023) *terra: Spatial Data Analysis*. Available at: https://CRAN.R-project.org/package=terra.

Hoecker, T. et al. (2025) 'TopoTerra'. OSF. Available at: https://doi.org/10.17605/OSF.IO/W6JVK.

Holden, Z.A. *et al.* (2011) 'Empirical modeling of spatial and temporal variation in warm season nocturnal air temperatures in two North Idaho mountain ranges, USA', *Agricultural and Forest Meteorology*, 151(3), pp. 261–269. Available at: https://doi.org/10.1016/j.agrformet.2010.10.006.

Holden, Z.A. *et al.* (2019) 'TOPOFIRE: A Topographically Resolved Wildfire Danger and Drought Monitoring System for the Conterminous United States', *Bulletin of the American Meteorological Society*, 100(9), pp. 1607–1613. Available at: https://doi.org/10.1175/BAMS-D-18-0178.1.

Huang, Y. *et al.* (2020) 'Effect of preseason diurnal temperature range on the start of vegetation growing season in the Northern Hemisphere', *Ecological Indicators*, 112, p. 106161. Available at: https://doi.org/10.1016/j.ecolind.2020.106161.

Kane, V.R. *et al.* (2015) 'Water balance and topography predict fire and forest structure patterns', *Forest Ecology and Management*, 338, pp. 1–13. Available at: https://doi.org/10.1016/j.foreco.2014.10.038.

Keddy, P.A. and Laughlin, D.C. (2021) *A framework for community ecology: species pools, filters and traits*. Cambridge University Press.

Keeley, J.E., van Mantgem, P. and Falk, D.A. (2019) 'Fire, climate and changing forests', *Nature Plants*, 5(8), pp. 774–775. Available at: https://doi.org/10.1038/s41477-019-0485-x.

Kemppinen, J. *et al.* (2024) 'Microclimate, an important part of ecology and biogeography', *Global Ecology and Biogeography*, 33(6), p. e13834. Available at: https://doi.org/10.1111/geb.13834.

Klinges, D.H. *et al.* (2022) 'MCERA5: Driving microclimate models with ERA5 global gridded climate data', *Methods in Ecology and Evolution*, 13(7), pp. 1402–1411. Available at: https://doi.org/10.1111/2041-210X.13877.

Klinges, D.H. *et al.* (2024) 'Proximal microclimate: Moving beyond spatiotemporal resolution improves ecological predictions', *Global Ecology and Biogeography*, p. e13884. Available at: https://doi.org/10.1111/geb.13884.

Lauritsen, R.G. and Rogers, J.C. (2012) 'U.S. Diurnal Temperature Range Variability and Regional Causal Mechanisms, 1901–2002', *Journal of Climate*, 25(20), pp. 7216–7231. Available at: https://doi.org/10.1175/JCLI-D-11-00429.1.

Lüdecke, D. et al. (2021) 'performance: An R Package for Assessment, Comparison and Testing

of Statistical Models', *Journal of Open Source Software*, 6(60), p. 3139. Available at: https://doi.org/10.21105/joss.03139.

Maclean, I.M.D. and Early, R. (2023) 'Macroclimate data overestimate range shifts of plants in response to climate change', *Nature Climate Change*, 13(5), pp. 484–490. Available at: https://doi.org/10.1038/s41558-023-01650-3.

Maclean, I.M.D. and Klinges, D.H. (2021) 'Microclimc: A mechanistic model of above, below and within-canopy microclimate', *Ecological Modelling*, 451, p. 109567. Available at: https://doi.org/10.1016/j.ecolmodel.2021.109567.

Maclean, I.M.D., Mosedale, J.R. and Bennie, J.J. (2019) 'Microclima: An R package for modelling meso- and microclimate', *Methods in Ecology and Evolution*. Edited by S. McMahon, 10(2), pp. 280–290. Available at: https://doi.org/10.1111/2041-210X.13093.

Mahood, A. (2024) 'topomicro: Topography and Microclimate Tools'. Available at: www.github.com/admahood/topomicro.

Mahood, A. (2025) 'Data and code for "Diurnal temperature range drives understory plant community composition in micro-climatically complex temperate forests". Zenodo. Available at: https://doi.org/10.5281/zenodo.14768076.

Mahood, A.L. *et al.* (2024) 'Soil climate underpins year effects driving divergent outcomes in semi-arid cropland-to-grassland restoration', *Ecosphere*, 15(10), p. e70042. Available at: https://doi.org/10.1002/ecs2.70042.

Mahood, A.L. and Balch, J.K. (2019) 'Repeated fires reduce plant diversity in low-elevation Wyoming big sagebrush ecosystems (1984–2014)', *Ecosphere*, 10(2), p. e02591. Available at: https://doi.org/10.1002/ecs2.2591.

Mahrt, L. (2006) 'Variation of Surface Air Temperature in Complex Terrain', *Journal of Applied Meteorology and Climatology*, 45(11), pp. 1481–1493. Available at: https://doi.org/10.1175/JAM2419.1.

Mahrt, L. (2022) 'Horizontal Variations of Nocturnal Temperature and Turbulence Over Microtopography', *Boundary-Layer Meteorology*, 184(3), pp. 401–422. Available at: https://doi.org/10.1007/s10546-022-00721-w.

Man, M. *et al.* (2022) 'Can high-resolution topography and forest canopy structure substitute microclimate measurements? Bryophytes say no', *Science of The Total Environment*, 821, p. 153377. Available at: https://doi.org/10.1016/j.scitotenv.2022.153377.

Manasa S, L. *et al.* (2022) 'Overview of Cold Stress Regulation in Plants', *The Botanical Review*, 88(3), pp. 359–387. Available at: https://doi.org/10.1007/s12229-021-09267-x.

Marchin, R.M. *et al.* (2022) 'Extreme heat increases stomatal conductance and drought-induced mortality risk in vulnerable plant species', *Global Change Biology*, 28(3), pp. 1133–1146. Available at: https://doi.org/10.1111/gcb.15976.

McCune, B. and Keon, D. (2002) 'Equations for Potential Annual Direct Incident Radiation and Heat Load', *Journal of Vegetation Science*, 13(4), pp. 603–606.

Minchin, P.R. (1987) 'An evaluation of the relative robustness of techniques for ecological ordination', *Vegetatio*, 69, pp. 89–107.

Morelli, T.L. *et al.* (2016) 'Managing Climate Change Refugia for Climate Adaptation', *PLOS ONE*. Edited by H. Rebelo, 11(8), p. e0159909. Available at: https://doi.org/10.1371/journal.pone.0159909.

Mu, Q. *et al.* (2022) 'Phenotypic plasticity in plant height shaped by interaction between genetic loci and diurnal temperature range', *New Phytologist*, 233(4), pp. 1768–1779. Available at: https://doi.org/10.1111/nph.17904.

Muldavin, E. and Tonne, P. (2003) 'A vegetation survey and preliminary ecological assessment of Valles Caldera National Preserve, New Mexico, Los Alamos, NM, Valles Caldera Trust, Final Report, Cooperative Agreement No. 01CRAG0014. Available online from the New Mexico Natural Heritage Program', Available online from the New Mexico Natural Heritage Program at http://nmnhp. unm. edu/vlibrary/pubs_ns/nmnhp_pubs_ns. php [Preprint].

Myster, J. and Moe, R. (1995) 'Effect of diurnal temperature alternations on plant morphology in some greenhouse crops—a mini review', *Scientia Horticulturae*, 62(4), pp. 205–215. Available at: https://doi.org/10.1016/0304-4238(95)00783-P.

Novick, K.A., Oishi, A.C. and Miniat, C.F. (2016) 'Cold air drainage flows subsidize montane valley ecosystem productivity', *Global Change Biology*, 22(12), pp. 4014–4027. Available at: https://doi.org/10.1111/gcb.13320.

Nychka, D. *et al.* (2021) 'fields: Tools for spatial data'. Boulder, CO, USA: University Corporation for Atmospheric Research. Available at: https://github.com/dnychka/fieldsRPackage.

Oksanen, J. *et al.* (2022) *vegan: Community Ecology Package*. Available at: https://CRAN.R-project.org/package=vegan.

Pastore, M.A. *et al.* (2024) 'Frequent and strong cold-air pooling drives temperate forest composition', *Ecology and Evolution*, 14(4), p. e11126. Available at: https://doi.org/10.1002/ece3.11126.

Patiño, J. *et al.* (2023) 'Spatial resolution impacts projected plant responses to climate change on topographically complex islands', *Diversity and Distributions*, 29(10), pp. 1245–1262. Available at: https://doi.org/10.1111/ddi.13757.

Piñeiro, G. *et al.* (2008) 'How to evaluate models: Observed vs. predicted or predicted vs. observed?', *Ecological Modelling*, 216(3–4), pp. 316–322. Available at: https://doi.org/10.1016/j.ecolmodel.2008.05.006.

Platt, R.V., Chapman, T.B. and Balch, J.K. (2024) 'Fire refugia are robust across Western US forested ecoregions, 1986–2021', *Environmental Research Letters*, 19(1), p. 014044. Available at: https://doi.org/10.1088/1748-9326/ad11bf.

PRISM Climate Group (2024) *PRISM Gridded Climate Data*. Available at: https://prism.oregonstate.edu.

R Core Team (2021) R: A Language and Environment for Statistical Computing. Vienna, Austria:

R Foundation for Statistical Computing. Available at: https://www.R-project.org/.

Rodman, K.C. *et al.* (2023) 'Refuge-yeah or refuge-nah? Predicting locations of forest resistance and recruitment in a fiery world', *Global Change Biology*, 29(24), pp. 7029–7050. Available at: https://doi.org/10.1111/gcb.16939.

Ruehr, N.K. *et al.* (2015) 'Water availability as dominant control of heat stress responses in two contrasting tree species', *Tree Physiology*. Edited by F. Meinzer, p. tpv102. Available at: https://doi.org/10.1093/treephys/tpv102.

Rupp, D.E. *et al.* (2021) 'Influence of anthropogenic greenhouse gases on the propensity for nocturnal cold-air drainage', *Theoretical and Applied Climatology*, 146(1–2), pp. 231–241. Available at: https://doi.org/10.1007/s00704-021-03712-y.

Said, S.E. and Dickey, D.A. (1984) 'Testing for unit roots in autoregressive-moving average models of unknown order', *Biometrika*, 71(3), pp. 599–607. Available at: https://doi.org/10.1093/biomet/71.3.599.

Seager, R. *et al.* (2015) 'Climatology, Variability, and Trends in the U.S. Vapor Pressure Deficit, an Important Fire-Related Meteorological Quantity', *Journal of Applied Meteorology and Climatology*, 54(6), pp. 1121–1141. Available at: https://doi.org/10.1175/JAMC-D-14-0321.1.

Suggitt, A.J. *et al.* (2018) 'Extinction risk from climate change is reduced by microclimatic buffering', *Nature Climate Change*, 8(8), pp. 713–717. Available at: https://doi.org/10.1038/s41558-018-0231-9.

Sun, X. et al. (2019) 'Global diurnal temperature range (DTR) changes since 1901', *Climate Dynamics*, 52(5–6), pp. 3343–3356. Available at: https://doi.org/10.1007/s00382-018-4329-6.

Trapletti, A. and Hornik, K. (2024) *tseries: Time Series Analysis and Computational Finance*. Available at: https://CRAN.R-project.org/package=tseries.

Valles Caldera Trust (2011) VALLES CALDERA NATIONAL PRESERVE Existing Condition Report-Soils. Jemez Springs, NM.

Wang, F. *et al.* (2014) 'Diurnal temperature range variation and its causes in a semiarid region from 1957 to 2006', *International Journal of Climatology*, 34(2), pp. 343–354. Available at: https://doi.org/10.1002/joc.3690.

Western Regional Climate Center (2024) 'Valles Caldera National Preserve Climate Stations'. Available at: https://wrcc.dri.edu/vallescaldera/.

Supplemental Figures

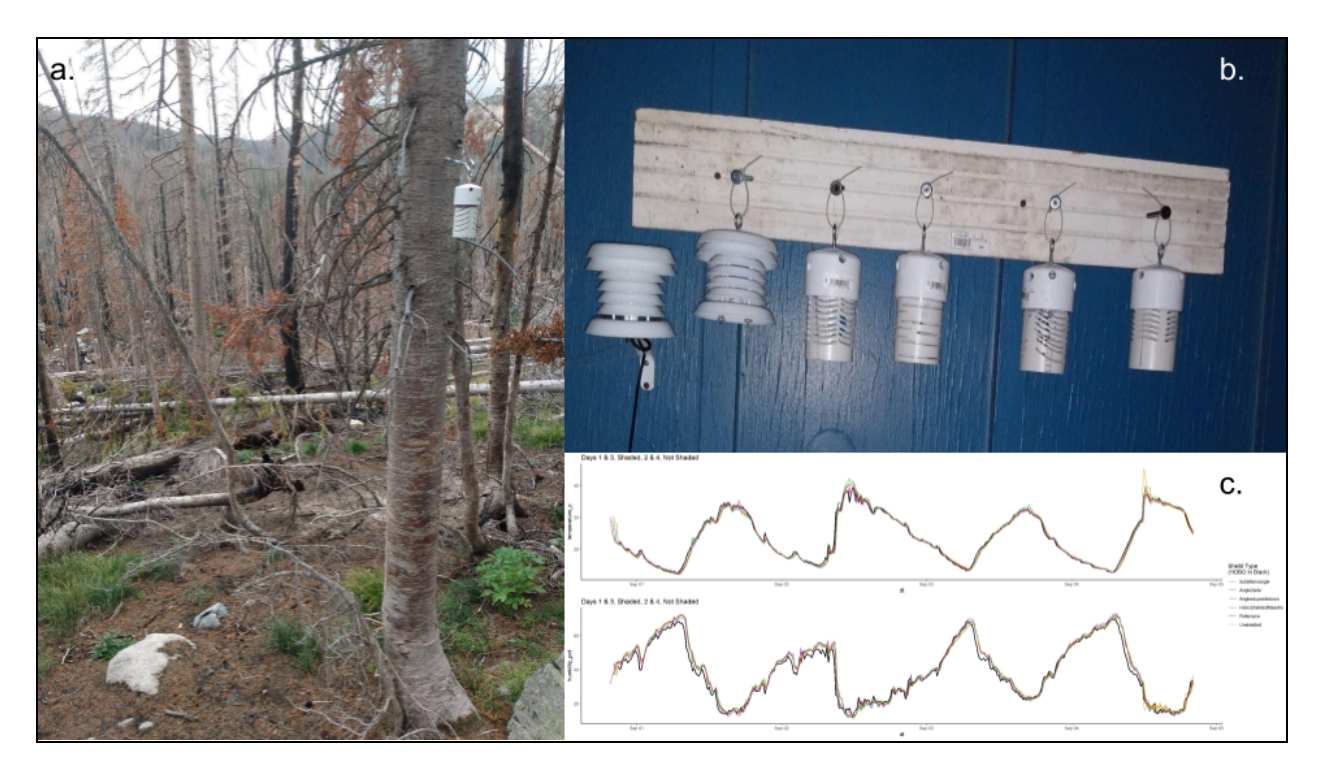


Figure S1. Sensors used and tests of radiation shields. In a, a sensor housed in the final design for radiation shield, attached to the north side of a tree. Panel b illustrates the testing of homemade radiation shields. The far left sensor was a HOBO RH/T sensor, second from the left was a Blue Maestro sensor housed in a HOBO radiation shield, and the four to the right were Blue Maestro sensors housed in different designs of our home-made shields. In c, a comparison of the data in the shade (Days 1 & 3) versus in sun (Days 2 & 4).

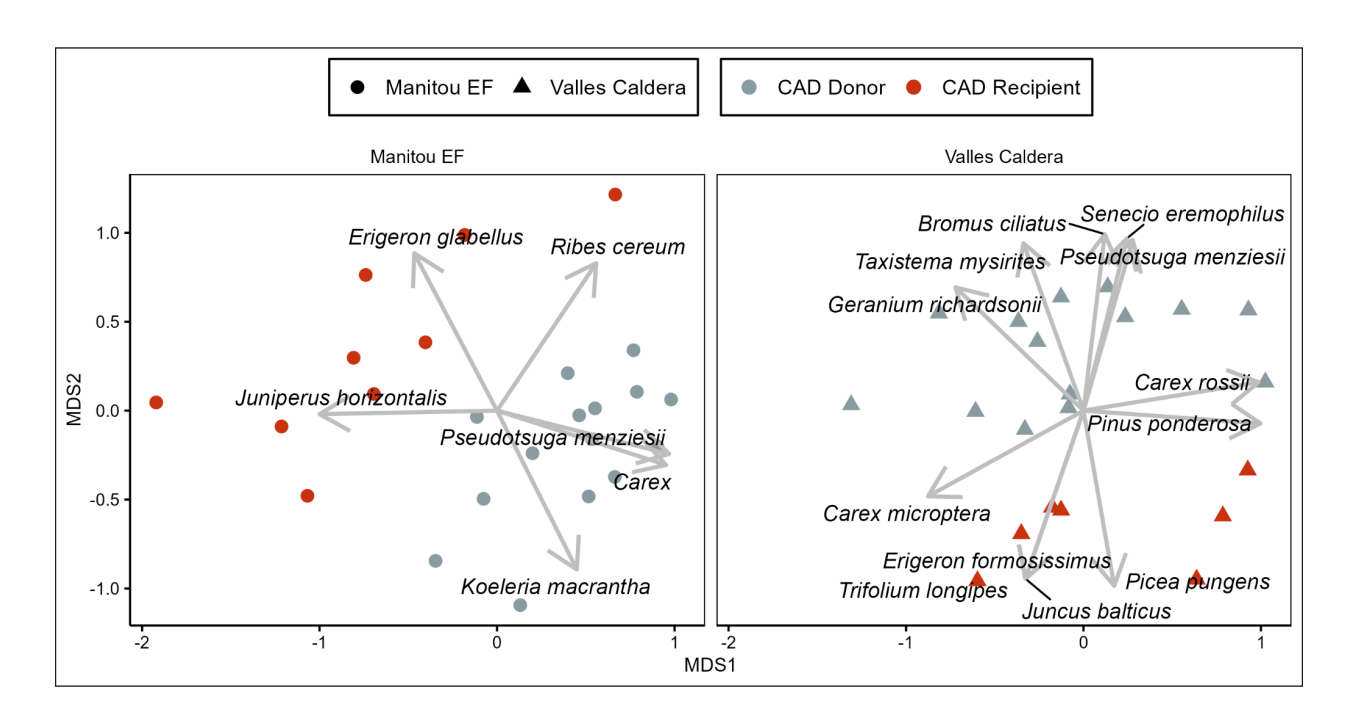


Figure S2: Species that were strongly correlated with the ordinations (p < 0.05; $R^2 > 0.4$)

Table S1. Understory species occurring at 5 or more plot locations at Maintou Experimental Forest

Species	Prevalence
Koeleria macrantha	18
Achillea millefolium	17
Carex sp	16
Arctostaphylos uva-ursi	15
Juniperus communis	15
Ribes cereum	14
Solidago missouriensis	13
Antennaria microphylla	12
Muhlenbergia montana	12
Geranium caespitosum	10
Allium cernuum	9
Heterotheca foliosa	9
Jamesia americana	9
Penstemon sp	9
Rosa woodsii	9
Thalictrum fendleri	9
Elymus elymoides	8
Geranium richardsonii	8
Artemisia ludoviciana	7
Campanula rotundifolia	7
Eremogone fendleri	7
Festuca arizonica	7
Fragaria vesca	7
Carex geyeri	6
Galium boreale	6
Holodiscus discolor	6
Poa fendleriana	6
Acer glabrum	5
Androsace septentrionalis	5
Boechera pendulina	5
Erigeron glabellus	5
Fragaria virginiana	5
Mertensia lanceolata	5
Potentilla hippiana	5
Sedum lanceolatum	5
Taraxacum officinale	5

Table S2. Understory species occurring at 5 or more plot locations at Valles Caldera

Species	Prevalence
Taraxacum officinale	14
Achillea millefolium	13
Bromus ciliatus	13
Poa pratensis	13
Koeleria macrantha	12
Taxistema mysirites	9
Bromus porteri	8
Carex rossii	8
Geranium richardsonii	8
Senecio eremophilus	8
Fragaria vesca	7
Fragaria virginiana	7
Lathyrus lanzwertii	7
Potentilla hippiana	7
Potentilla pulcherrima	7
Ribes sp	7
Carex microptera	6
Oreochrysum parryi	6
Trifolium repens	6
Vicia americana	6
Viola canadensis	6
Agrostis scabra	5
Artemisia franseroides	5
Festuca thurberi	5

Table S3. Model Coefficients for the diversity model.

term	estimate	std.error	CI 0.025	CI 0.975
(Intercept)	2.899	0.059	2.775	3.013
DTR threshold x CAD Recipient	-0.223	0.105	-0.429	-0.02
Site: Valles Caldera	0.231	0.081	0.073	0.396
DTR threshold x CAD Recipient x Site: Valles Caldera	0.101	0.145	-0.182	0.393

Table S4. Structural equation model coefficients.

Response	e Predicto	Estimate	Standard Error	DF	Critical Value	p-value	Standardized Estimate
nspp	tdelta	-0.041	0.0146	41	-2.8094	0.005**	-0.3892
nspp	twi	0.0275	0.012	41	2.2866	0.0222*	0.2356
nspp	rel_elv	0	3.00E-04	41	-0.1516	0.8795	-0.0197
tdelta	elevation	ı -0.0122	0.0016	42	-7.7592	0***	-0.7016
tdelta	twi	0.3772	0.1002	42	3.7637	5.00E-04***	0.3403